https://doi.org/10.5194/egusphere-2024-2267
Preprint. Discussion started: 18 September 2024

Use of simple analytical solutions in the calibration of Shallow Water Equations debris flow models

Riccardo Bonomelli[1], Marco Pilotti[1], Gabriele Farina[1]

[1]DICATAM, Università degli Studi di Brescia, Brescia, 25123, Italy

Correspondence to: Riccardo Bonomelli (riccardo.bonomelli@unibs.it)

Abstract. Modelling debris flow propagation requires numerical models able to describe the main characteristics of the flow, like velocity or inundation extent. Due to the complex physics involved, every numerical model is dependent from a set of parameters whose influence on the results is often not evident. In this contribution we propose simple analytical solutions based on the monophasic Shallow Water Equations for some of the most used rheological models (O'Brien & Julien, Voellmy, Bingham and Bagnold) implemented in monophasic (FLO-2D, RAMMS, HEC-RAS, TELEMAC-2D) and biphasic commercial software (TRENT2D). These simplified solutions and their asymptotic uniform-flow like relationship are useful on one hand to speed up the calibration process, limiting the need to perform multiple simulations with unrealistic set of parameters and on the other hand as a benchmark for existing numerical methods. To further guide the calibration, a Sobol's sensitivity analysis has been performed to highlight which parameters of the considered equations have the most influence on the flow velocity. Finally, as an example of application, the proposed methodology is validated on a real debris flow event occurred in Italy.

1 Introduction

The computation of hydraulic hazard related to debris flow is of paramount importance for risk mapping in mountain areas. In spite of their limitations with respect to models which better respect the physics of the process like the two-phase models (e.g. Pitman and Le, 2005; Armanini et al., 2009; Pudasaini and Fischer, 2020) and multi-phase models (Pudasaini and Mergili, 2019), monophasic ones, based on Shallow Water Equations, are still widely used in the practice and they can be effective (e.g. Rickenmann et al., 2006) when suitably calibrated (e.g. Stancanelli and Foti, 2015). However, apart from theoretical limitations, when the adopted rheological relation is multiparametric, its calibration is not straightforward. In the following, dealing only with depth-averaged models, we will use the term "rheology" as a synonym for friction law or bottom stress. In the widely used FLO-2D model, an empirical quadratic rheological relation (O'Brien & Julien, 1988) is used, as a function of several parameters and of the sediment concentration. Simpler relations are the one proposed by Voellmy (Voellmy, 1955), implemented in the RAMMS model (Christen et al., 2010) and in HEC-RAS Mud and Debris Flow (US Army Corps of Engineers, 2023) or the Bingham-like rheology (Malet et al., 2005; Begueria et al., 2009; Sauthier et al., 2015). The calibration of the rheological parameters is typically done, for past events, either by using experimental measurements or, more commonly, by reproducing the extension of mapped inundated areas, the distribution of the debris

https://doi.org/10.5194/egusphere-2024-2267
Preprint. Discussion started: 18 September 2024

flow volume and the timing of the propagation, all of which information may not be available. Moreover, the calibration is typically done empirically, by exploring the multiparametric space without a precise insight on the impact of a specific parameter set until the whole simulation has been accomplished. However, over the last 10 years debris-flow monitoring techniques have greatly improved (e.g. Hürlimann et al., 2019) and many monitoring systems have been installed worldwide that can provide observations on debris flow velocity and the corresponding stage along a channel reach. The same information can also be provided by occasional recording and we believe that can be extremely valuable in constraining the calibration process. In this paper we propose to use a simple analytical solution for the uniform motion of a monophasic debris-flow with a general quadratic equation rheology along a channel of constant slope, to obtain the following results: 1) simplify the calibration by providing a priori insights on the role of the different rheological parameters on the modelled debris-flow velocity, 2) identify a characteristic time of the model, to be used to evaluate the distance needed to reach the theoretical normal flow condition, and, in more general terms, to adapt the flow to bed-slope changes, 3) identify possible parameter combinations that lead to flow slow-down, 4) investigate the different parameters sensitivity on the process. As a final fall-out of this research, we show that two parameters of the widely used FLO-2D model are not observable, i.e. their value can't be separately estimated from observations, (e.g. Sorooshian & Gupta, 1983), so leading to a 20% reduction of the number of parameters to be identified for this widely used model. We believe that these observations can be used to simplify the calibration process when field data are scarce. As an example, we applied the described results to a real debris flow event occurred in Ono San Pietro, Italy, where footage of the debris flow was available.

2 Governing equations

The 1D Shallow Water Equations

$$\begin{aligned} &h_t + (hu)_x = 0 \\ &(hu)_t + \left(hu^2 + \frac{1}{2}gh^2\right)_x = gh(S_b - S_f) \end{aligned} \tag{1}$$

where h $[m]$ is the fluid depth, u $[m\ s^{-1}]$ is the flow velocity along the x direction, g $[m\ s^{-2}]$ is the acceleration of gravity, S_b $[-]$ is the bed slope and S_f $[-]$ is the friction slope, can be used to model the propagation of a monophasic non-newtonian debris flow on a rigid bed if a suitable model is selected for the friction slope. Although a steady state condition is rare in natural debris flows, some field and laboratory measurements of debris flow velocity in a confined channel (e.g. Takahashi, 1991; Hungr, 2000; Lanzoni et al., 2017) have shown that, where the flow is fully developed (Bernard et al., 2023) velocity records can show limited variations in terms of depth and velocity over distance. This constant velocity can be reproduced by a simple physically-based relationship of the asymptotic velocity of a debris layer with constant depth h (measured normally with respect to the bottom), destabilized along an incline of constant slope. To account for cross-sections of limited width in a channel, it is possible to replace h with the hydraulic radius (Perla et al., 1980). This analogy also provides a characteristic time for fluid acceleration. Using a Voellmy's rheology, this approach was originally proposed for a snow avalanches

https://doi.org/10.5194/egusphere-2024-2267
Preprint. Discussion started: 18 September 2024

(Voellmy, 1955; Perla et al., 1980; Pudasaini and Hutter, 2007) and, more recently, for a debris flow (Hergarten & Robl, 2015). The transient velocity u of the debris layer can be obtained by simplifying system (1) for a layer of infinite length (or alternatively, by adopting a Lagrangian framework) as

$$u'(t) = g(S_b - S_f) \tag{2}$$

Equation (2) can be solved analytically if the equation of the friction's slope S_f make it possible. A rather general rheology model is the quadratic one, according to which S_f can be written as a function of velocity as

$$S_f = Pu^2 + Qu + R \tag{3}$$

where P, Q and R are functions of the flow depth or fluid properties. Combining Eq. (2) and (3) leads to a Riccati equation

$$\begin{aligned} &u'(t) = A\,u^2(t) + B\,u(t) + C \\ &A = -g\,P; \quad B = -g\,Q; \quad C = g\sin\vartheta - gR \end{aligned} \tag{4}$$

Pudasaini & Krautblatter (2022) proposed a series of analytical solutions to estimate landslide velocity as a function of rather general rheologies where the linear term in the velocity is not included ($B = 0$) because this term is negligible compared to the quadratic one when extremely fast flows are considered (Perla et al., 1980). Models in which $B \neq 0$ were considered by Salm (1966) and Nishimura and Maeno (1989) but only for snow avalanches. However, the linear term B may be important considering debris flows. Eq. (4) has some interesting properties. For instance, it is clear that C must be $\neq 0$ if the motion starts from rest, as assumed in the following. The asymptotical velocity u_∞ is provided by solving the quadratic equation obtained by setting $u'(t) = 0$ in Eq. (4). Accordingly, the discriminant $B^2 - 4AC$ must be positive for a uniform velocity to exist. When $A \neq 0$, the solution $u(t)$ of Eq. (4) can then be obtained analytically with a standard integration of Riccati's equation, leading to

$$\begin{aligned} &u(t) = -\tfrac{B}{2A} + \sqrt{|\varphi|}\tanh\left[\tfrac{(t+\varepsilon)}{T}\right] \\ &\varepsilon = -\frac{1}{A\sqrt{|\varphi|}}\operatorname{atanh}\left(\frac{B}{2A\sqrt{|\varphi|}}\right) \\ &T = \frac{2}{\sqrt{B^2 - 4AC}}; \quad \varphi = \frac{4AC - B^2}{4A^2} \end{aligned} \tag{5}$$

where ε is a constant of integration computed using the condition that the initial velocity is zero, $u(0) = 0$, and T is the characteristic time of the flow, which measures how quickly the velocity reaches its asymptotic value. The solution for the Voellmy model, investigated by Herganten and Robl (2015) and Pudasaini and Krautblatter (2022), implemented in the widely used RAMMS software (Christen et al., 2010), can be obtained by Eq. (5) when $B = 0$. When $A = 0$ and $B \neq 0$ (a case corresponding to a Bingham's rheology) another simple solution can be obtained from (4) by separation of variables as

https://doi.org/10.5194/egusphere-2024-2267
Preprint. Discussion started: 18 September 2024

$$u(t) = \frac{C}{B}(e^{Bt} - 1)$$
$$T = \frac{1}{|B|} \quad (6)$$

Finally, if $A = B = 0$ (a case corresponding to a pure velocity-independent Coulomb's friction) then the straightforward solution is

$$u(t) = C\,t \quad (7)$$

where the characteristic time does not exist anymore, reflecting the property that the flow will infinitely accelerate.

3 Application to different rheological models

The quadratic model (3) is used to describe the rheology of debris flows according to a monophasic approximation in some widely used numerical models. In the following sections the analytical solutions (5) and (6) will be used to show how the parameters of (3) affect the flow asymptotic velocity u_∞ and the characteristic time T, showing how field observations can constrain the parameters identification. Furthermore, a sensitivity analysis will provide additional insights on the rheological parameters which most impact the uniform velocity theoretically reached by the flow.

3.1 O'Brien and Julien's rheology

One of the most used commercial software for the assessment of debris flow hazard is FLO-2D (O'Brien et al., 1993). To model debris flows, FLO-2D uses an ad-hoc rheology proposed by O'Brien and Julien (1988), as

$$S_f = \frac{\tau_y}{\gamma_m\,h} + \frac{K\,\eta\,u}{8\,\gamma_m\,h^2} + \frac{n_t^2 u^2}{h^{4/3}} \quad (8)$$

where τ_y $[N\,m^{-2}]$ is the yield stress of the granular material, γ_m $[N\,m^{-3}]$ is the equivalent fluid specific weight, K $[-]$ is a resistance parameter for laminar flow, η $[Pa\ s]$ is the viscosity and n_t $[s\,m^{-1/3}]$ is the turbulent Manning's coefficient. Specific weight, viscosity, yield stress and turbulent Manning's coefficient are functions of the volumetric sediment concentration C_v $[-]$ according to the relations (O'Brien and Julien, 1988)

$$\eta = \alpha_1 e^{\beta_1 C_v};\quad \tau_y = \alpha_2 e^{\beta_2 C_v}$$
$$n_t = 0.0538\,n\,e^{6.0896\,C_v};\quad \gamma_s = C_v\,\gamma_m + (1 - C_v)\,\gamma_w \quad (9)$$

where α_1 $[Pa\ s]$, $\alpha_2[Pa]$, $\beta_1[-]$ and β_2 $[-]$ are empirical coefficient that could be defined by laboratory experiments (O'Brien and Julien, 1988), n $[s\,m^{-1/3}]$ is the Manning's coefficient while γ_m $[N\,m^{-3}]$ and γ_w $[N\,m^{-3}]$ are the sediment and water specific weight respectively. Accordingly, apart from Manning's coefficient and sediment specific weight, that can be more easily identified, the model is a function of the six parameters $\alpha_1, \beta_1, \alpha_2, \beta_2, K$ and C_v. The solution (5) can be used with the following meaning of the coefficients

$$A = -\frac{g\,n_t^2}{h^{4/3}};\quad B = -\frac{g\,K\,\eta}{8\,\gamma_m\,h^2};\quad C = g\sin\vartheta - \frac{g\tau_y}{\gamma_m h} \quad (10)$$

and the asymptotic velocity u_∞ is given by

https://doi.org/10.5194/egusphere-2024-2267
Preprint. Discussion started: 18 September 2024

$$u_\infty = \left[-\frac{K\,\eta}{8\,\gamma_m\,h^2} + \sqrt{\left(\frac{K\,\eta}{8\,\gamma_m h^2}\right)^2 + 4\frac{n_t^2}{h^{4/3}}\left(\sin\vartheta - \frac{\tau_y}{\gamma_m h}\right)} \right] \frac{h^{4/3}}{2n_t^2} \tag{11}$$

whereas the characteristic time is

$$T = \frac{2}{\sqrt{\left(\frac{K\,\eta\,g}{8\,\gamma_m h^2}\right)^2 + 4\frac{g\,n_t^2}{h^{4/3}}\left(\sin\vartheta - \frac{\tau_y}{\gamma_m h}\right)}} \tag{12}$$

By inspection of Eq. (11) and (12) one can obtain some interesting insights that can be useful for the calibration of a FLO-2D based model:

- K always appears multiplied by η and thus K and α_1 are not indipendent and can be considered as a single parameter. Accordingly, the number of degrees of freedom of the O'Brien parametrization during calibration is reduced by 20%.
- The asymptotic velocity is positive if and only if

$$\sin\vartheta - \frac{\tau_y}{\gamma_m h} > 0 \tag{13}$$

that is, among others, a non-linear function of the concentration C_v, since τ_y and γ_m depend on the concentration. This condition can also be regarded as one controlling the progressive flow deceleration of the modelled equivalent fluid.

We believe that Eq. (11) and (12) can be useful for the calibration of the numerical model. As an example, Fig. 1 shows the dimensionless analytical solution for the "Aspen Pit 1" parameters set (O'Brien and Julien, 1988), considering typical values $h = 1\ m$ and $\vartheta = 20°$. For this set of values, $u_\infty = 4.85\ m\ s^{-1}$ and $T = 2.89\ s$. Accordingly, $u(T)/u_\infty = 0.86$. The maximum sediment concentration for the flow to develop a uniform velocity is computed by solving Eq. (13), i.e. $C_v = 0.49$; by exceeding this limiting concentration, the flow will slow down and stop.

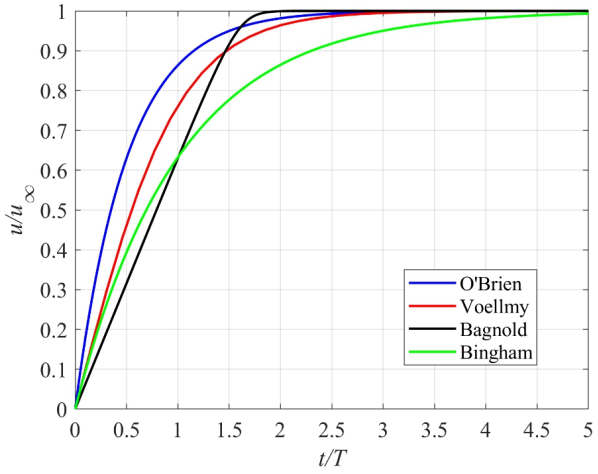

Figure 1. Dimensionless analytical solution for 4 different rheological models. The solution (5) using the O'Brien rheology is shown in blue using the "Aspen Pit 1" parameters set with $\gamma_w = 9\,810\ N\ m^{-3}$ (water specific weight), $\gamma_s = 26\,500\ N\ m^{-3}$ (specific weight of sediments), $n = 0.033\ s\ m^{-1/3}$ and $K = 2285$. The solid red line is the analytical solution (16) for the Voellmy rheology using $\mu = 0.1$ and $\xi = 1000\ m\ s^{-2}$. The solid green line shows the solution computed using Bingham frictional law (20) with $\tau_c = 200\ Pa, \gamma_m = 15\,000\ N\ m^{-3}$ and $\eta = 90\ Pa\ s$. Finally the black line is the numerical solution using Bagnold frictional law with

https://doi.org/10.5194/egusphere-2024-2267
Preprint. Discussion started: 18 September 2024

$\rho_s = 2\,300\ kg\ m^3$, $\rho_w = 1\,000\ kg\ m^{-3}$, $\phi_d = 35°$, $Y = 40$, $\beta = 1$ and $c_b = 0.65$. In this case, being a numerical solution, there is no formula for the characteristic time, and the time at which the flow reaches 63% of the uniform velocity has been arbitrarily selected as the characteristic time for the normalization. In all cases the debris flow layer h is equal to 1 m and the channel slope is 20°.

	$T\ [s]$	$u_\infty\ [m\ s^{-1}]$	$u(T)/u_\infty\ [-]$
O'Brien	2.89	4.85	0.86
Voellmy	6.47	15.74	0.76
Bagnold	0.52	2.77	0.63
Bingham	5.32	16.74	0.63

Table 1. Numerical summary of the characteristic time T, terminal velocity u_∞ and ratio between the velocity for $t = T$, $u(T)$, and the terminal one u_∞ for all rheological models described.

Despite the large number of parameters to be calibrated, the O'Brien rheology is widely used in monophasic numerical models to replicate past debris flow events (e.g. Cesca and D'Agostino, 2008; Lin et al., 2011; Wu et al., 2013; Stancanelli and Foti, 2015; Wang et al., 2024). Calibration of parameters is performed either a posteriori, i.e. using observations of depositional height or maximum velocity, or using rheological investigations (Boniello et al., 2010). In this process one may wonder which parameters have the greatest impact on the simulation results, a type of information that is difficult to know a priori, even when they appear explicitly like in Eq. (11). Although this information can be obtained by performing multiple simulations that encompass the range of variation of each parameter of the friction law, this way remains impractical if one does not use parallelization techniques as done by Zegers et al. (2020). In the following, in order to shed light on the relevance of each parameter on the model output and its interaction with other parameters, a Sobol's global sensitivity analysis is performed (Sobol, 1993). After assuming the value of ϑ and h, Sobol's analysis quantifies the amount of variance that each parameter contributed to the unconditional variance of the model output (Nossent et al., 2011) and has been frequently used in environmental (Saltelli and Annoni, 2010; Estrada and Diaz, 2010) and hydrological modelling (Pappenberger et al., 2008). The amount of variance relative to the total variance, called Sobol's sensitivity index, can be attributed either to a single parameter (so-called, first order index) or to the interaction of a single parameter with respect to the others (total order index). For instance, in the case of Eq. (11), being the model a function of seven parameters, i.e. α_k (given by the product of α_1 and K, as observed above), $\beta_1, \alpha_2, \beta_2, n, C_v$ and γ_s, the computation of Sobol's indexes could be accomplished by a Monte Carlo method. However, from the computational point of view, it can be better to evaluate the first and total order indexes according to the estimators recently proposed by Azzini et al. (2021), due to their simplicity in implementation. These estimators provide a better performance with respect to the ones originally introduced by Saltelli (2002). For each model evaluation, the set of parameters has been selected using the latin hypercube sampler (Azzini et al., 2021). Each parameter is assumed to vary uniformly inside the range shown in Table 2, obtained considering typical values from the literature. The uniform probability distribution reflects the absence of information about the flow being modelled but, if laboratory or field measurements are available, other parameter distributions can be used. The velocity distributions obtained from random parameter sets used to perform the Sobol analysis corresponding to each rheological model are reported in Fig. 2. A conservative random sample size of 50 000 parameter sets has been used, repeating the analysis 100 times to ensure the robustness of the Sobol indices shown in Fig. 3, where $h = 1\ m$ and $\vartheta = 20°$.

https://doi.org/10.5194/egusphere-2024-2267
Preprint. Discussion started: 18 September 2024

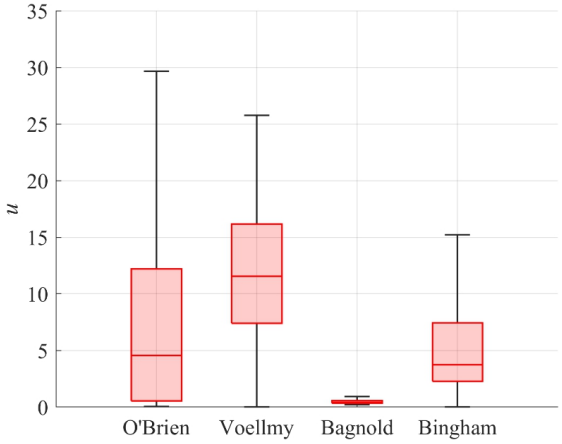

Figure 2. Uniform velocity boxplot distribution for the 4 rheological models used to perform Sobol sensitivity analysis ($h = 1\ m$, $\vartheta = 20°$). For each graph the solid line represents the median value across the whole distribution, the rectangular box covers the range from the lower quartile (25%) to the upper quartile (75%) and the whiskers show the non-outlier maximum (the maximum data value which is not an outlier) and minimum (the minimum data value which is not an outlier). Here a point is classified as an outlier if it lies more than 1.5 times the interquartile range away from the top or bottom of the red-shaded rectangle.

Parameter	Minimum	Maximum	Units	Reference
α_1	$3 \cdot 10^{-5}$	$6.4 \cdot 10^{-3}$	$Pa\ s$	Sosio et al., (2007)
β_1	6.2	33.1	–	Zegers et al., (2020)
α_2	$7.1 \cdot 10^{-5}$	0.0181	Pa	Zegers et al., (2020)
β_2	16.9	29.8	–	O'Brien and Julien, (1988)
C_v	0.2	0.55	–	-
n	0.01	0.2	$s\ m^{-1/3}$	Zegers et al., (2020)
K	24	2285	–	O'Brien and Garcia, (2009)
α_k	$7.2 \cdot 10^{-4}$	14.62	$Pa\ s$	O'Brien & Garcia, (2009); Sosio et al., (2007)
γ_s	18	25	$kN\ m^{-3}$	-

Table 2. Variation range for the parameters tested in the Sobol analysis.

As shown in Fig. 3, the first-order Sobol index highlights that the most influential parameters are C_v, β_1 and n, in order of importance. C_v is able, by itself, to explain around 35% of the variance of the terminal velocity, as one could expect considering that C_v influences all the terms in Eq. (11) whereas the other parameters affect just a single term of the equations. High model sensitivity to β_1 (almost 20%) confirms other findings in literature (Zegers et al., 2020). The sensitivity on the Manning's coefficient (around 13%) reflects the importance of surface roughness and associated turbulent friction. This is not in line with the findings of Zegers et al. (2020), in which model results are insensitive to Manning's roughness coefficient. This can be explained considering that the reference velocity considered by Zegers et al. (2020), that appears quadratically in the term where the Manning's coefficient appears, is around $1\ m\ s^{-1}$, in contrast with the wider range of velocities considered in this study (see Fig. 2). Parameters $\alpha_k, \alpha_2, \beta_2$ and γ_s appear to be less important in terms of the terminal velocity.

https://doi.org/10.5194/egusphere-2024-2267
Preprint. Discussion started: 18 September 2024

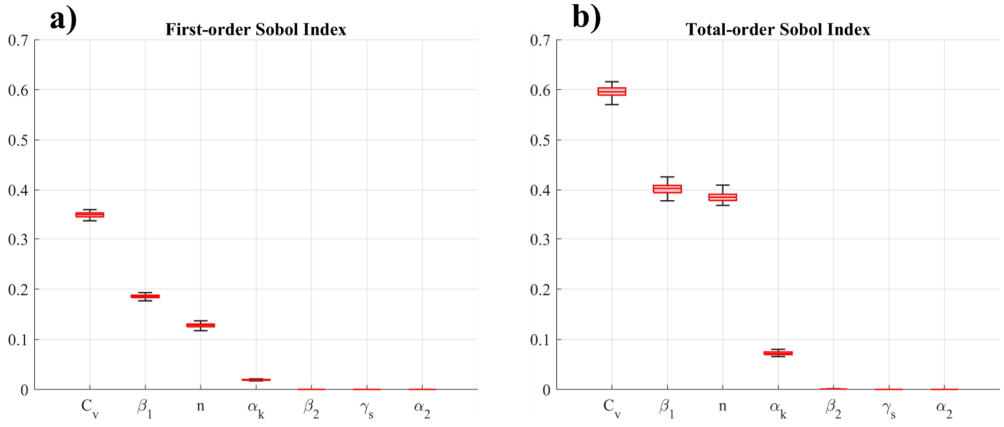

Figure 3. Boxplot of the first-order Sobol index (a) and total order index (b) for the parameters of the O'Brien rheology, ordered in terms of importance.

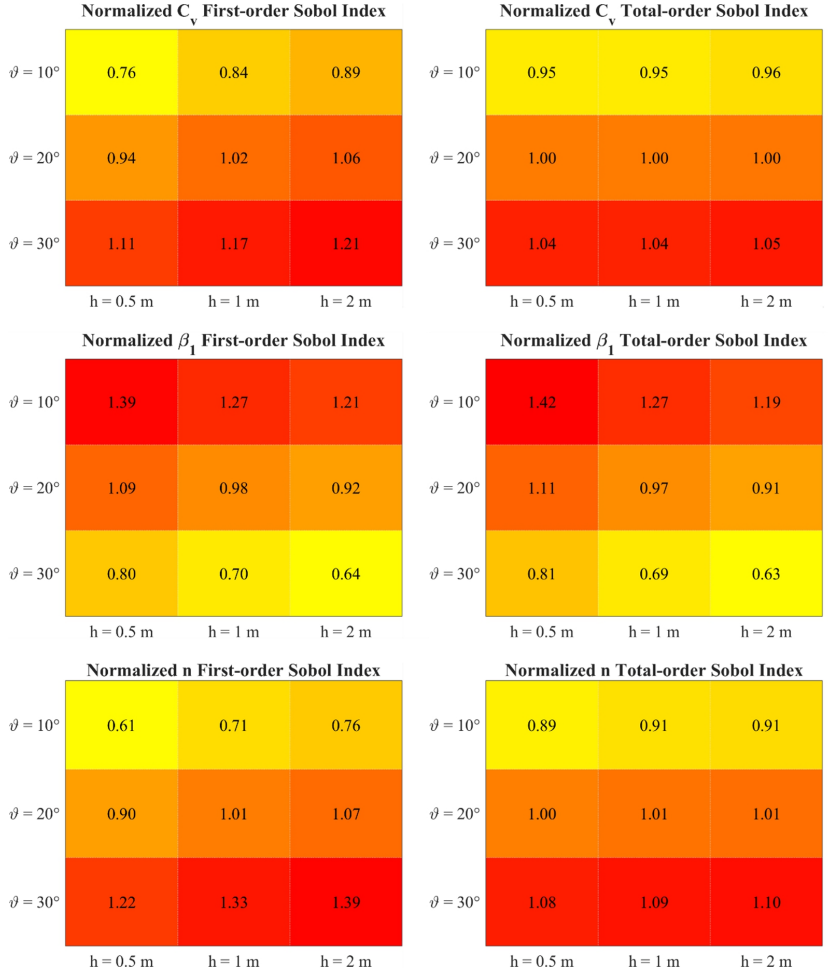

175 **Figure 4. First-order (left) and total-order (right) Sobol index for the parameters C_v, β_1 and n as a function of different values of ϑ and h. Each entry of the matrix represents the first- (total-) order Sobol index computed using the corresponding (h, ϑ) couple, then divided by the average index over the whole matrix. The average first-order (total-order) Sobol indexes for C_v, β_1 and n are 0.34 (0.6), 0.19 (0.41) and 0.13 (0.38) respectively.**

https://doi.org/10.5194/egusphere-2024-2267
Preprint. Discussion started: 18 September 2024

Globally, the sum of the first order Sobol indexes can explain 68% of the variance of the model meaning that the remainder of the variance is due to the nonlinearity of the model, i.e. the variance generated by a combination of parameters. Total-order indexes reveals the importance of the interactions between C_v, β_1 and n. As observed above, the results of the sensitivity analysis are valid for a given couple of the fluid depth h and channel slope ϑ: therefore the following analysis has been repeated to explore the variation of the Sobol indexes as a function of (h, ϑ). Fig. 4 shows the Sobol indexes for C_v, β_1 and n, normalized by dividing each index by its average value across the whole matrix. The colour shading shows the growing direction for each index. As one can observe, the first-order Sobol index of C_v and n is a growing function of h and ϑ whereas their total-order index is mostly a growing function of ϑ. Considering β_1, both the first-order and total-order Sobol indexes show that for growing values of h and ϑ the sensitivity of the uniform velocity decreases, suggesting the growing importance of viscosity for small fluid depths or channel slope.

3.2 Voellmy's rheology

The Voellmy rheology (Voellmy, 1955) splits the total basal friction into a velocity independent dry-Coulomb term proportional to the normal stress at the flow bottom and a velocity dependent friction (Salm, 1993). This simple friction law is implemented in several numerical software, e.g. RAMMS (Christen et al., 2010), HEC-RAS Mud and Debris Flow (US Army Corps of Engineers, 2023) and FLATModel (Medina et al., 2007). The Voellmy's friction law is given by

$$S_f = \mu \cos\vartheta + \frac{u^2}{\xi\, h} \tag{14}$$

where μ $[-]$ is a Coulomb friction coefficient and ξ $[m\ s^{-2}]$ is a turbulent friction coefficient. The analytical solution to eq. (2) is given by Eq. (5) using the following coefficients

$$A = -\frac{g}{\xi\, h};\quad B = 0;\quad C = g \sin\vartheta - g\, \mu \cos\vartheta \tag{15}$$

obtaining the solution suggested by Voellmy (1955) and Hergarten and Robl (2015)

$$u(t) = u_\infty \tanh\left(\frac{t}{T}\right)$$
$$u_\infty = \sqrt{\xi h(\sin\vartheta - \mu\cos\vartheta)};\quad T = \frac{\xi\, h}{g\, u_\infty} \tag{16}$$

Eq. (16) is a simple and interesting piece of information to evaluate the appropriateness of the parameters used to propagate the debris flow being modelled. Once again by inspection of the terminal velocity of Eq. (16) one can conclude that the flow can approach a uniform condition only when $\tan\vartheta > \mu$, meaning that the slope of the channel must be higher than the friction coefficient. This reflects the simple observation that the friction force is larger than the gravity component and therefore a balance between the two, i.e. the steady state velocity, is impossible. Assuming invariance of the parameters during the motion, this condition can be used to calibrate the friction parameters μ that must be upper limited by the local slope angle in the inception area and lower limited by the local slope angle where the debris flow has stopped its propagation. The analytical solution (16) is shown in Fig. 1 in correspondence of the parameters set $\mu = 0.1$, $\xi = 1\,000\ m\ s^{-2}, h = 1\ m$ and $\vartheta = 20°$. After a characteristic time $(6.47\ s)$ the flow approaches a velocity which is 76% of the terminal one $(15.74\ m\ s^{-1})$. Performing the Sobol sensitivity analysis described above yields the results reported in Table 3, where the first line is the variation range explored in the analysis and $h = 1\ m$ and $\vartheta = 20°$. The indices highlight a balanced sensitivity of the uniform velocity to both parameters, with μ scoring slightly higher both in terms of the first- and total-order indices.

https://doi.org/10.5194/egusphere-2024-2267
Preprint. Discussion started: 18 September 2024

	ξ	μ
Range	$50 - 2\,000\ m\,s^{-2}$	$0.01 - 0.36$
First-order index	0.40	0.55
Total-order index	0.44	0.60

Table 3. Summary of the Sobol sensitivity analysis obtained with a fluid depth of 1 m and a channel slope of 20°. The parameter's range is taken from RAMMS user manual.

Repeating the analysis for different values of h and ϑ shows little variation in terms of the computed sensitivity indices (both first- and total-order ones); therefore the indices reported in Table 3 are representative of the whole spectrum of variation of h and ϑ.

3.3 Bagnold's rheology

Bagnold's rheology (1954) modified by Takahashi (1978) on the basis of experimental data and valid for stony-type debris flow is used, for instance, inside the TRENT2D software (Rosatti and Begnudelli, 2013):

$$S_f = \frac{25}{4}\frac{\rho_s}{\rho_w}\sin\phi_d \frac{\lambda^2}{Y^2(1 + C_v\,\Delta_s)\,g\,h}u^2$$
$$\lambda = \left[(c_b/C_v)^{1/3} - 1\right]^{-1};\quad \Delta_s = \frac{\rho_s - \rho_w}{\rho_w};\quad C_v = c_b\beta\frac{u^2}{gh} \tag{17}$$

where $\rho_s\ [kg\ m^{-3}]$ is the density of the sediments, $\rho_w\ [kg\ m^{-3}]$ is the density of water, $\phi_d\ [°]$ is the friction angle of the sediments, $Y\ [-]$ is the submergence parameter, Δ_s is the submerged relative density of the sediments, $c_b\ [-]$ is the maximum concentration of the mixture in static conditions, $C_v\ [-]$ is the concentration of the mixture and β is a transport parameter to be calibrated. Although the submergence parameter depends on other factors, following Rosatti and Begnudelli (2013) we kept it as a calibration parameter. Due to the function λ, which depends non-linearly on the velocity, a simple analytical expression of the solution of (2) is no longer obtainable. Similarly, a simple closed-form expression for the uniform velocity can't be obtained, due to the non-integer exponents present inside Eq. (17). Accordingly, to compare the results with previous models, we solved Eq. (2) numerically, by using a finite difference method. The solution is shown in Fig. 1, for $\rho_s = 2\,300\ kg\ m^3, \rho_w = 1\,000\ kg\ m^{-3}, \phi_d = 35°, Y = 40, \beta = 1$, $c_b = 0.65$, $h = 1\ m$ and $\vartheta = 20°$. For this combination, it is characterized by a uniform velocity of $2.77\ m\ s^{-1}$ and a characteristic time of $0.52\ s$. Being a numerical solution, no expression for the characteristic time is available, and the time when the flow reaches 63% of the uniform velocity has been arbitrarily regarded as the characteristic time, in analogy with an exponential decay. Contrary to the rheological models studied so far, Bagnold's model provides a uniform velocity for every choice of the parameters, when $\vartheta > 0$. The Sobol has been repeated for the Bagnold's rheology exploring the parameters range shown in Table 4, taken from literature (e.g. Stancanelli and Foti, 2015).

	β	Y	ϕ_d	ρ_s	c_b
Range	$0.1 - 100$	$1 - 50$	$20 - 45°$	$1\,800 - 2\,500\ kg\ m^{-3}$	$0.4 - 0.65$
First-order index	0.95	0.01	$9 \cdot 10^{-5}$	$3 \cdot 10^{-6}$	$3 \cdot 10^{-6}$
Total-order index	0.98	0.04	$5 \cdot 10^{-4}$	$3 \cdot 10^{-5}$	10^{-5}

Table 4. Summary of the Sobol sensitivity analysis obtained with a fluid depth of 1 m and a channel slope of 20°.

The indexes of Table 4 show that the most important parameter is β, which by itself is able to explain more than 90% of the variance, while the others show limited influence on the uniform velocity. Repeating the analysis for different values of h and ϑ shows little to no variation in terms of the computed sensitivity indices (both first- and total-order ones); therefore the indices shown in Table 4 are representative for the whole spectrum of variation of h and ϑ. Furthermore, considering the

https://doi.org/10.5194/egusphere-2024-2267
Preprint. Discussion started: 18 September 2024

uniform velocity distributions showed in Fig. 2 for the different rheological models it is possible to notice that the Bagnold rheology is characterized by a narrow field of variation of the velocity ($0 - 3\ m\ s^{-1}$) with respect to the other rheologies. This finding is in line with other comparative works in literature (e.g. Stancanelli & Foti, 2015) where it is observed that FLO-2D (O'Brien rheology) can predict velocities during a general simulation which are considerably higher ($1.5 - 20\ m\ s^{-1}$) compared with the TRENT2D (Bagnold rheology) ones ($1 - 2\ m\ s^{-1}$) on the same simulation.

3.4 Bingham's rheology

The Bingham (1922) rheology is another commonly adopted model for debris flow propagation (Malet et al. 2005; Begueria et al., 2009), implemented, for instance, inside the TELEMAC-2D software (TELEMAC-2D User Manual, 2017). The main assumption in the Bingham model of laminar flow regime of viscoplastic materials with a constant value of yield strength and viscosity is especially valid in flows with high fine fraction (Abraham et al., 2022). Using the shear stress equation reported in Coussot (1997), a simplified Bingham expression of shear stress has been used to derive the value of the friction slope term, as proposed by (Abraham et al., 2022):

$$S_f = \frac{3\,\tau_c}{2\,\gamma_m\,h\cos\vartheta} + \frac{3\,\eta\,u}{\gamma_m h^2\cos\vartheta} \tag{18}$$

where $\tau_c\ [Pa]$ is the constant yield strength due to cohesion of soil in the static case, $\eta\ [Pa\ s]$ is the viscosity parameter and $\gamma_m\ [N\ m^{-3}]$ is the specific weight of the mixture. Using the following coefficients

$$A = 0; \quad B = -\frac{3\,\eta\,g}{\gamma_m h^2\cos\vartheta}; \quad C = g\sin\vartheta - \frac{3\,\tau_c\,g}{2\,\gamma_m\,h\cos\vartheta} \tag{19}$$

from Eq. (6) one can obtain the analytical solution

$$u(t) = u_\infty\left(e^{-\frac{3\,\eta\,g}{\gamma_m h^2\cos\vartheta}t} - 1\right)$$
$$u_\infty = \frac{\gamma_m h^2\cos\vartheta}{3\,\eta}\left(\sin\vartheta - \frac{3\,\tau_c}{2\,\gamma_m\,h\cos\vartheta}\right) \tag{20}$$
$$T = \frac{\gamma_m h^2\cos\vartheta}{3\,\eta\,g}$$

Finally, the flow will approach a terminal velocity if the quantity inside the brackets of Eq. (20) is positive, i.e. if

$$\sin\vartheta\cos\vartheta > \frac{3\,\tau_c}{2\,\gamma_m\,h} \tag{21}$$

providing a simple criterion which may be useful during the calibration process of numerical models. Fig. 1 plots the analytical solution Eq. (20) using $\tau_c = 200\ Pa, \eta = 90\ Pa\ s, \gamma_m = 15\,000\ N\ m^{-3}, h = 1\ m$ and $\vartheta = 20°$. After a characteristic time of $5.32\ s$ the flow reaches a velocity of $16.74\ m\ s^{-1}$ which is 63% of the terminal velocity. Interestingly, the parameter τ_c does not influence the characteristic time of the flow, but only the terminal velocity. Table 5 shows the results obtained by performing Sobol sensitivity analysis in the range taken from Phillips and Davies (1991) and using $h = 1\ m$ and $\vartheta = 20°$. The indices highlight a high sensitivity of the uniform velocity to the viscosity η, while the other parameters show negligible influence on the model's output. This finding is consistent with what already found using the O'Brien rheology, i.e. that parameters that control viscosity strongly influences the uniform velocity.

https://doi.org/10.5194/egusphere-2024-2267
Preprint. Discussion started: 18 September 2024

	η	τ	γ_m
Range	$1 - 10^3\ Pa\ s$	$0.1 - 10^3\ N\ m^{-2}$	$16 - 23\ kN\ m^{-3}$
First-order index	0.83	$6 \cdot 10^{-3}$	10^{-3}
Total-order index	0.99	0.14	0.018

Table 5. Summary of the Sobol sensitivity analysis, assuming a fluid depth of 1 m and a channel slope of 20°.

Repeating the analysis for different values of h and ϑ shows little to no variation in terms of the computed sensitivity indices (both first- and total-order ones). Accordingly the indices reported in Table 5 are representative of the whole spectrum of variation of h and ϑ.

4 Application and discussion

The proposed analytical solutions can be applied to simplify the calibration of parameters when some insights on the expected debris flow velocity are available, as shown in the following with reference to the debris flow that occurred in the Blè basin in Valle Camonica valley, in the Central Italian Alps (Lombardia Region). On August 16, 2021, a debris flow was triggered by an intense rainfall of 40 mm in 1 hour, caused by a localized storm cell moving west to east (Berti et al., 2023). The event mobilized a total volume of about 60 000 m^3 and travelled along the channel for about 2 kilometres before covering a local road with debris and boulders. A monitoring station (Berti et al., 2023) provided video footage of the debris flow through a known cross-section.

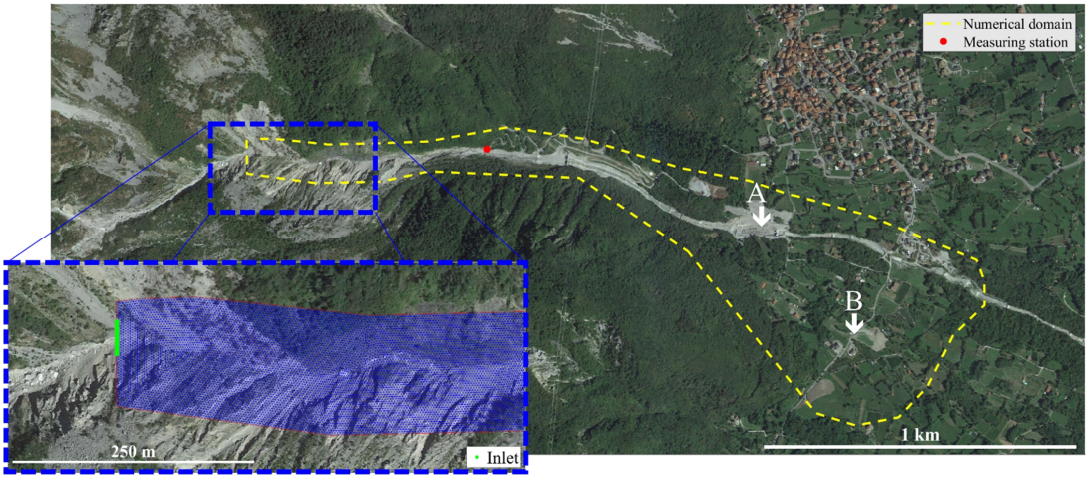

Figure 5. Map view of the study area. The yellow dashed line highlights the computational domain used in this numerical simulation, the red dot illustrates the position of the recording station while the dashed blue line shows an enlargement of the inlet cross section (depicted in green) as well as the unstructured mesh adopted for the simulation. Locations A and B indicate the main areas where the debris flow deposited, (© Google Earth 2019).

Using video footage and cross-section geometry, Berti et al. (2023) combined two free Matlab tools (PIVlab, Thielicke and René, 2021 and RiveR, Patalano et al., 2017) in order to estimate the peak flow velocity and discharge. The obtained peak flow velocity and discharge are 4.4 $m\ s^{-1}$ and 224 $m^3\ s^{-1}$ respectively during the first surge and 5.4 $m\ s^{-1}$ and 227 $m^3\ s^{-1}$ during the second one (Berti et al., 2023). Based on the volume of the event and peak discharge, the reconstructed solid hydrograph shown in Fig. 6 was adopted as a boundary condition. The two-peak structure of the hydrograph was obtained by fixing the peaks (both assumed of 227 $m^3\ s^{-1}$ for simplicity) as well as the time lag between the first surge and the second one (about 2 minutes), with the constrain on the overall duration of the event of about 10

https://doi.org/10.5194/egusphere-2024-2267
Preprint. Discussion started: 18 September 2024

minutes. Considering the inertial nature of the debris flows in the Blè watershed, in the following the Voellmy model was used in the calibration process.

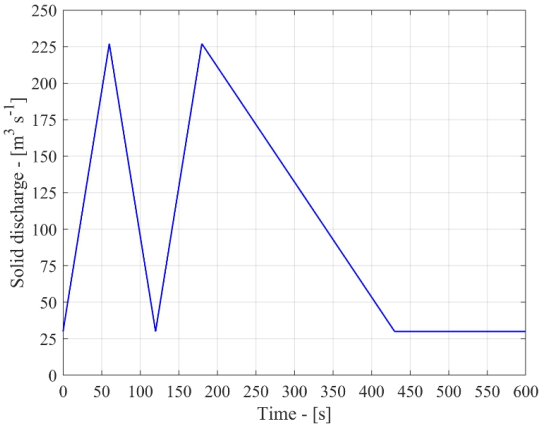

Figure 6. Solid discharge hydrograph used as a boundary condition for the Blè event. Two discharge peaks were observed during the event, approximately two minutes apart. This information, together with the total volume estimate provided, allowed to fix the shape of the hydrograph. A base flow of 30 $m^3\ s^{-1}$ was assumed after the analysis of the available video footage.

The Voellmy rheological model uses only two parameters: μ and ξ: the first one can be estimated using the local average slope in the main deposition area of the debris flow (locations A and B of Fig. 5), which has been evaluated to be around 14° based on the available DEM: accordingly, $\mu = 0.249$. Eq. (16) provides a first guess estimate for ξ, using the cross section geometry where the velocity was measured. Setting $u_\infty = 5.4\ m\ s^{-1}$, $h = 2\ m$ (Berti et al., 2023), $\mu = 0.249$ and computing the average slope at the measuring station, i.e. $\vartheta \approx 30°$, one can obtain a first guess for ξ

$$\xi = \frac{u_\infty^2}{h\,(\sin\vartheta - \mu\cos\vartheta)} \tag{22}$$

of about $52\ m\ s^{-2}$. The corresponding characteristic time, Eq. (16), is about $2\ s$, confirming that the debris flow rapidly adjusts itself to the local slope. Having determined two first-guess values for the rheological parameters, the numerical simulation can be performed to assess whether the depositional depths and extent reasonably match the observed ones. The Finite Volume SWE-based numerical scheme presented in Bonomelli et al. (2023), adapted for mountain area applications (Bonomelli and Pilotti, 2023; Bonomelli, 2024) was used to propagate the debris flow along the main channel of the catchment, with an unstructured triangular mesh consisting of 194 151 elements with an average distance of $1.63\ m$. The stopping criteria for propagation adopted by RAMMS (RAMMS manual, 2022) was implemented, which happened after 17 minutes of simulated time. Fig. 7 shows the simulated deposition map compared to the extent surveyed after the event (see the supplementary material for some photos of the event). The observed qualitative match is good and could be further improved to better reproduce the main characteristics of the event.

https://doi.org/10.5194/egusphere-2024-2267
Preprint. Discussion started: 18 September 2024

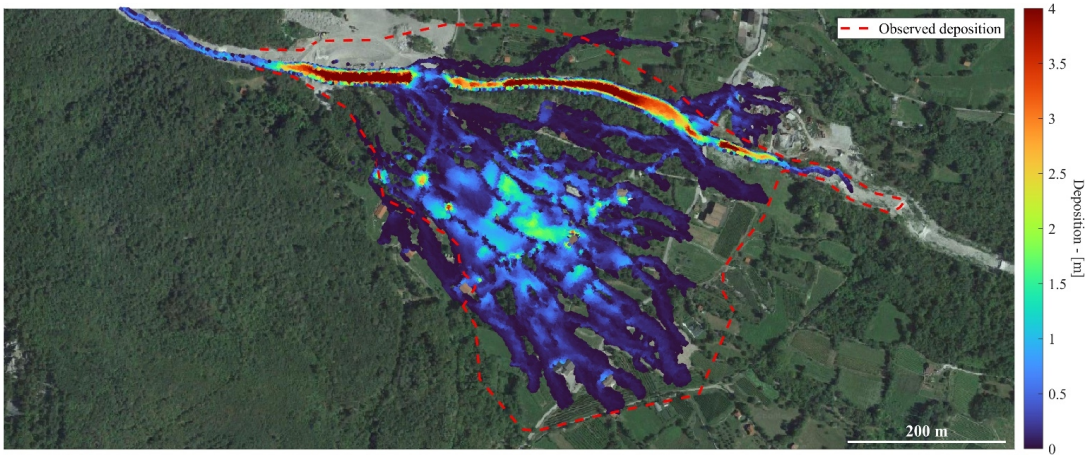

Figure 7. Deposition map at the end of the simulation using the Voellmy model with $\mu = 0.249$ and $\xi = 52\ m\ s^{-2}$ (© Google Earth 2019).

Fig. 8 shows the computed velocity profile at the measuring station in correspondence of the peak during the simulation. Quite interestingly, the identified ξ value, although obtained by a steady state formula, provides velocity during the transient process which are in the order of $5 - 6\ m\ s^{-1}$, confirming the role of the small characteristic time and the effectiveness of the simple analytical law adopted. The same figure also shows the higher velocity profile that would be obtained if the same input hydrograph were routed with the same μ but with a blind initial guess of ξ, selected in the middle of its documented range of variation.

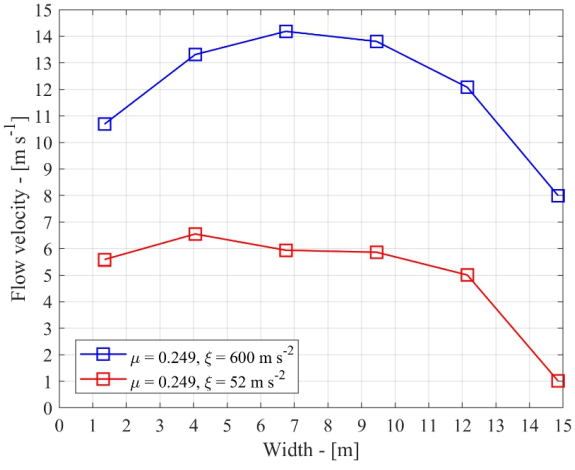

Figure 8. Peak flow velocity module at the measuring cross-section. The two profiles are obtained with the same μ value but different ξ. For blue squares, ξ was selected in the middle of its range of admissible values, while for red squares, the value of ξ was obtained using the proposed approach exploiting the available velocity measurement.

Accordingly, the proposed approach provides an effective initial guess for the rheological parameters of the Voellmy's model if a velocity measurement is available at a known cross-section, showing how a simple analytical law can speed up the calibration process. Using the Voellmy rheology, which has only two parameters, both can be constrained: however this methodology can be applied to any of the mentioned rheological models to reduce the number of parameters to be explored. In the case of the multiparametric O'Brien's rheology adopted in FLO-2D, this reduction acts synergistically with the observation that K always appears multiplied by α_1 in Eq. (11) and thus K and α_1 are not indipendent and can be considered

https://doi.org/10.5194/egusphere-2024-2267
Preprint. Discussion started: 18 September 2024

as a single parameter. This property, that to our knowledge has so far passed unnoticed in the vast literature on FLO-2D, is clearly shown by the simple example of Fig. 9, where the 1D profile for a dam break problem on a dry inclined slope for a debris flow described by the O'Brien & Julien rheology is shown. The profile is shown 30 s after starting from rest and is computed with two different parameter sets. The first is the mentioned Aspen pit 1 set and the second set is obtained from the first by switching the value of K and α_1. The numerical solution is computed solving the complete SWE in bottom-oriented coordinates, using the Finite Volume SWE-based numerical scheme by Bonomelli et al. (2023). As one can observe, there is no detectable difference between the two simulations. It is interesting to observe that using FLO-2D in similar tests, some differences were observed between the simulations, possibly due to other numerical features of that code.

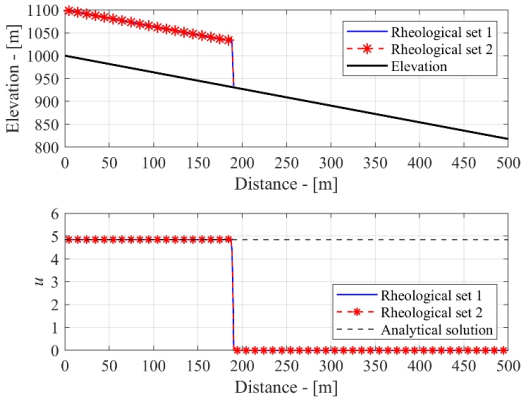

Figure 9. Numerical solution of a dam break problem on a sloping dry bed with O'Brien & Julien friction law. The initial condition is a constant fluid depth of 1 m in the first 100 m, while completely dry elsewhere. Boundary conditions used are a constant fluid depth upstream and transmissive boundary conditions downstream. The snapshot depicts the numerical solution 18 s after release with two rheological sets: 1) Aspen pit 1 and 2) Aspen pit 1 with $\alpha_1 = 2285\ Pa\ s$ and $K = 0.0036$. The dashed black line in the bottom panel depicts the transient analytical solution for the flow velocity showed in Eq. (5). In the top panel the fluid depth has been enlarged for graphical purposes.

Finally, another interesting use of Eq. (16) is as a uniform flow relation for the implementation of the inlet (or outlet) boundary condition (Hou et al, 2015) inside a numerical model. For instance, by rearranging Eq. (16) for the Voellmy rheological model one can easily obtain the incoming discharge as a function of the fluid depth

$$Q(h) = L\, h^{3/2} \sqrt{\xi\,(\sin\beta - \mu\cos\beta)} \tag{23}$$

where L is the inlet cross section width and β is the local channel inclination, which must exceed μ for the flow to occur. Similar relations can be obtained for the other rheological models described.

5 Conclusions

Although monophasic models like FLO-2D, RAMMS, HEC-RAS or TELEMAC-2D only provide a first-order approximation of the complex dynamics of debris flow propagation, they are widely used in the practice and strongly dependent on parameters that can be difficult to identify. This inevitably leads to a trial-and-error optimization that is computationally demanding. To limit this effort of "blind" simulations, it is practically useful to have some simple analytical solutions like Eq. (11), (12), (16) and (20) that, in presence of field measurements or other evidence, can be used to evaluate the normal flow velocity for a given parameters set. This velocity is a physical constrain that can be compared to the one expected or observed in the field. This procedure is shown with reference to the Blé test case where the Voellmy's model is used for the simulation. The proposed equations can also provide additional insights on the physical interplay between parameters, like the lack of observability of the O'Brien rheology with respect to K and α_1. These two parameters appear only in a multiplicative fashion within the equations and, accordingly, can be considered as a single parameter ($\alpha_k = \alpha_1\, K$),

https://doi.org/10.5194/egusphere-2024-2267
Preprint. Discussion started: 18 September 2024

reducing the degrees of freedom during the calibration process. This property, previously undocumented, is shown clearly in this paper with a simple numerical example. The Sobol sensitivity analysis is performed to highlight which parameters have a greater influence on the uniform velocity for each rheology, so further helping the calibration effort. Regarding O'Brien rheology, the most influential parameters are C_v (silt concentration), β_1 (exponential coefficient of the viscosity) and n (Manning's coefficient). For the Voellmy rheology each parameter is equally important. In the Bingham rheological model the viscosity parameter, i.e. η, dominates the magnitude of the uniform flow velocity. In both O'Brien and Bingham models, the viscosity that appears in the linear term in the velocity is very important. Finally, in the case of the Bagnold rheology, the most influential parameter in terms of the uniform velocity is the transport parameter, which traditionally is calibrated experimentally (Armanini et al., 2009). Accordingly, we believe that the proposed analytical solutions, together with the sensitivity analysis to the parameter involved, can be a significant help to guide the calibration of numerical models. While our results are limited to the analysis of a stage-discharge relation and of a characteristic time, so providing a single piece of information of a more complex picture, they are not confined to a particular case or geometry and accordingly have a wider applicability. Other possible uses of the proposed solutions (Eq. 11, 16 and 20) can be in the implementation of boundary conditions of numerical solver of monophasic models, in the computation of stage-discharge equations at a given cross-section (as showed in the Blé application, i.e. Eq. 23) or even, when coupled with a local mass balance, in the implementation of simplified kinematic routing schemes that could be used to provide back-of-the-envelope evaluations of the debris flow potential along the drainage network of a watershed.

Code availability

All software used in this research is available upon reasonable request to the authors.

Data availability

No datasets were used in this article.

Author contribution

RB and MP conceptualized the work, RB carried out the formal analysis and all authors contributed to write the paper, finally, GF reviewed and improved the paper.

Competing interests

The authors declare that they have no conflict of interest.

Acknowledgements

This research was accomplished within the project "Dynamics of debris flows in Val Camonica valley (Brescia): field monitoring of the Val Rabbia and Blè debris flow catchments", funded by Regione Lombardia, Italy. We thank Prof. Berti for leading the experimental activites in the Blè creek that provided the value of the measured debris-flow discharge used in the paper.

https://doi.org/10.5194/egusphere-2024-2267
Preprint. Discussion started: 18 September 2024

References

Abraham, M. T., Satyam, N., Pradhan, B. and Tian, H.: Debris flow simulation 2D (DFS 2D): Numerical modelling of debris flows and calibration of friction parameters, JRMGE, 14 (6), 1747-1760, https://doi.org/10.1016/j.jrmge.2022.01.004, 2022.

Armanini, A, Fraccarollo, L., Rosatti, G.: Two-dimensional simulation of debris flows in erodible channels, Comput. and Geosci, 35, 5, 993-1006, https://doi.org/10.1016/j.cageo.2007.11.008, 2009.

Azzini, I., Mara, T. A. and Rosati, R.: Comparison of two sets of Monte Carlo estimators of Sobol's indices, Environ. Model. Softw., 144, 105167, https://doi.org/10.1016/j.envsoft.2021.105167, 2021.

Bagnold, R. A.: Experiments on gravity-free dispersion of large solid spheres in a Newtonian fluid under shear, Proc. R. Soc. Lond. A, 225(1160):49-63, https://doi.org/10.1098/rspa.1954.0186, 1954.

Beguería, S., Van Asch, Th. W. J., Malet, J.-P., and Gröndahl, S.: A GIS-based numerical model for simulating the kinematics of mud and debris flows over complex terrain, Nat. Hazards Earth Syst. Sci., 9, 1897–1909, https://doi.org/10.5194/nhess-9-1897-2009, 2009.

Bernard, M., Barbini, M., Boreggio, M., Biassuzzi, K. and Gregoretti, C.: Deposition areas: an effective solution for the reduction of the sediment volume transported by stony debris flows on the high-sloping reach of channels incising fans and debris cones. Earth Surf. Process. Landf., 49, 2, https://doi.org/10.1002/esp.5727, 2023.

Berti, M., Schimmel, A., Coviello, V., Venturelli, M., Albertelli, L., Beretta, L., Brardioni, F., Ceriani, M., Pilotti, M., Ranzi, R., Redaelli, M., Scotti, R., Simoni, A., Turconi, L. and Luino, F.: Characterization of a debris flow event using an affordable monitoring system, 8th International Conference on Debris Flow Hazard and Mitigation, Torino, https://doi.org/10.1051/e3sconf/202341503004, 2023.

Bingham, E. C.: Fluidity and plasticity, McGraw-Hill, New York, 439, 1922.

Boniello, M. A., Calligaris, C., Lapasin, R., and Zini, L.: Rheological investigation and simulation of a debris-flow event in the Fella watershed, Nat. Hazards Earth Syst. Sci., 10, 989–997, https://doi.org/10.5194/nhess-10-989-2010, 2010.

Bonomelli, R., Farina, G., Pilotti, M., Molinari, D. and Ballio, F.: Historical comparison of the damage caused by the propagation of a dam break wave in a prealpine valley, J. Hydrol. Reg. Stud., 48, 101467, https://doi.org/10.1016/j.ejrh.2023.101467, 2023.

Bonomelli, R. and Pilotti, M.: A multi-rheological finite volume scheme on unstructured grid for debris flow propagation, 15th Congress INTERPRAEVENT 2022 Taiwan, 2023.

Bonomelli, R.: An enhanced modelling approach for debris flow inception and propagation, PhD thesis, 2024.

Cesca, M. and D'Agostino, V.: Comparison between FLO-2D and RAMMS in debris-flow modelling: a case study in the Dolomites, Monitoring, Simulation, Prevention and Remediation of Dense and Debris Flow II, WIT Press, 2008.

Christen, M., Kowalski, J. and Bartelt, P.: RAMMS: numerical simulation of dense snow avalanches in three-dimensional terrain, Cold Reg. Sci. Technol., 63, 1-14, https://doi.org/10.1016/j.coldregions.2010.04.005, 2014.

Coussot, P.: Mudflow Rheology and Dynamics, IAHR Monograph, 1997.

Estrada, V. and Diaz, M. S.: Global sensitivity analysis in the development of first principle-based eutrophication models. Environ. Model. Softw., 25, 1539-1551, https://doi.org/10.1016/j.envsoft.2010.06.009, 2010.

Hergarten, S. and Robl, J.: Modelling rapid mass movements using the shallow water equations in Cartesian coordinates, Nat. Hazards Earth Syst. Sci., 15, 671–685, https://doi.org/10.5194/nhess-15-671-2015, 2015.

Hou, J., Liang, Q., Zhang, H. and Hinkelmann, R.: An efficient unstructured MUSCL scheme for solving the 2D shallow water equations, Environ. Model. Softw., 66, 131-152, https://doi.org/10.1016/j.envsoft.2014.12.007, 2015

Hungr, O.: Analysis of debris flow surges using the theory of uniformly progressive flow, Earth Surf. Process. Landf., 25, 483-495, https://doi.org/10.1002/(SICI)1096-9837(200005)25:5<483::AID-ESP76>3.0.CO;2-Z, 2000.

https://doi.org/10.5194/egusphere-2024-2267
Preprint. Discussion started: 18 September 2024

Hürlimann, M., Coviello, V., Bel, C., Guo, X., Berti, M., Graf, C., Hübl, J., Miyata, S., Smith, J. B., Yin, H., Debris-flow monitoring and warning: Review and examples, Earth-Science Reviews, Volume 199, 102981, ISSN 0012-8252, https://doi.org/10.1016/j.earscirev.2019.102981, 2019.

Lanzoni, S., Gregoretti, C. and Stancanelli, L. M.: Coarse-grained debris flow dynamics on erodible beds, J. Geophys. Res. Earth Surf, 122, 592-614, https://doi.org/10.1002/2016JF004046, 2017.

Lin, J. Y., Yang, M. D., Lin, B. R. and Lin, P. S.: Risk assessment of debris flows in Songhe Stream, Taiwan, Eng. Geol., 123, 100–112, https://doi.org/10.1016/j.enggeo.2011.07.003, 2011.

Malet, J. P., Laigle, D., Remaître and Maquaire, O.: Triggering conditions and mobility of debris flows associated with complex earthflows, Geomorphology, 66, 215-235, https://doi.org/10.1016/j.geomorph.2004.09.014, 2005.

Medina, V., Hürlimann, M. and Bateman, A.: Application of FLATModel, a 2D finite volume code, to debris flows in the northeastern part of the Iberian Peninsula, Landslides, 5, 127-142, https://doi.org/10.1007/s10346-007-0102-3, 2007.

Nishimura, K. and Maeno, N.: Contribution of viscous forces to avalanche dynamics, Ann. Glaciol., 13, 1989.

Nossent, J., Elsen, P. and Bauwens, W.: Sobol sensitivity analysis of a complex environmental model, Environ. Model. Softw., 26, 1515-1525, https://doi.org/10.1016/j.envsoft.2011.08.010, 2011.

O'Brien, J. S. and Garcia, R.: FLO-2D Reference manual, available at: https://www.flo-2d.com/ (last access: 1 March 2019), 2009.

O'Brien, J. S., Julien, P. Y. and Fullerton, W. T.: Two-dimensional water flood and mudflow simulation, J. Hydraul. Eng, ASCE, 119(2), 244-259, https://doi.org/10.1061/(ASCE)0733-9429(1993)119:2(244), 1993.

O'Brien, J. S. and Julien, P. Y.: Laboratory analysis of mudflow properties, J. Hydraul. Eng., 114, 8, https://doi.org/10.1061/(ASCE)0733-9429(1988)114:8(877), 1988.

Pappenberger, F., Bartholmes, J., Thielen, J., Cloke, H. L., Buizza, R. and de Roo, A.: New dimensions in early flood warning across the globe using grand-ensemble weather predictions, Geophys. Res. Lett., 35, 10, https://doi.org/10.1029/2008GL033837, 2008.

Patalano, A., Garcia, C. M. and Rodriguez, A.: Rectification of image velocity results (RIVeR): A simple and user-friendly toolbox for large scale water surface Particle Image Velocimetry (PIV) and Particle Tracking Velocimetry (PTV), Comput. Geosci., 109, 323-330, https://doi.org/10.1016/j.cageo.2017.07.009, 2017.

Perla, R., Cheng, T. T., and McClung, D. M.: A two–parameter model of snow–avalanche motion, J. Glaciol., 26 (94), 197–207, https://doi.org/10.1017/s002214300001073x, 1980.

Pitman, E. B. and Le, L.: A two-fluid model for avalanche and debris flows, Philos. Transact. A Math. Phys. Eng. Sci., 363, 1573–1601, https://doi.org/10.1098/rsta.2005.1596, 2005.

Phillips, C. J. and Davies, T. R. H.: Determining rheological parameters of debris flow material, Geomorphology, 4, 101-110, https://doi.org/10.1016/0169-555X(91)90022-3, 1991.

Pudasaini, S. P. and Hutter, K.: Avalanche dynamics, Springer Berlin, 2007.

Pudasaini, S. P. and Mergili, M.: A multi-phase mass flow model. J. Geophys. Res. Earth Surf. 124, 2920–2942, https://doi.org/10.1029/2019JF005204, 2019.

Pudasaini, S. P. and Fischer, J. T.: A mechanical erosion model for two-phase mass flows, Int. J. Multiph. Flow 132, 103416, https://doi.org/10.1016/j.ijmultiphaseflow.2020.103416, 2020.

Pudasaini, S. P. and Krautblatter, M.: The landslide velocity, Earth Surf. Dynam., 10, 165–189, https://doi.org/10.5194/esurf-10-165-2022, 2022.

RAMMS::DEBRISFLOW User Manual: A numerical model for debris flows in research and practise, 2022.

Rickenmann, D., Laigle, D., McArdell, B.W. and Hübl, J.: Comparison of 2D debris-flow simulation models with field events, Comput. Geosci., 10, 241-264, https://doi.org/10.1007/s10596-005-9021-3, 2006.

https://doi.org/10.5194/egusphere-2024-2267
Preprint. Discussion started: 18 September 2024

Rosatti, G. and Begnudelli, L.: Two-dimensional simulation of debris flows over mobile bed: Enhancing the TRENT2D model by using a well-balanced Generalized Roe-type solver, Comput. Fluids, 71, 179-195, https://doi.org/10.1016/j.compfluid.2012.10.006, 2013.

Salm, B.: Contribution to avalanche dynamics, international association of scientific, hydrology publication 69 (Symposium at Davos 1965—Scientific aspects of snow and ice avalanches), pp 199–214, 1966.

Salm, B.: Flow, flow transition and runout distances of flowing avalanches, Ann. Glaciol., 221-226, https://doi.org/10.3189/S0260305500011551 , 1993.

Saltelli, A. and Annoni, P.: How to avoid a perfunctory sensitivity analysis, Environ. Model. Softw., 25, 1505-1517, https://doi.org/10.1016/j.envsoft.2010.04.012, 2010.

Saltelli, A.: Sensitivity Analysis for Importance Assessment. Risk Analysis, 22, 3, 2002.

Sobol, I. M.: Sensitivity estimates for nonlinear mathematical models, Mathematical Modelling and Computational Experiments, 4, 407-414, 1993.

Sauthier, C., Pirulli, M., Pisani, G., Scavia, C. & Labiouse V.: Numerical modelling of gravel unconstrained flow experiments with the DAN3D and RASH3D codes, Comput. Geosci., 85, 81-90, https://doi.org/10.1016/j.cageo.2015.09.008, 2015.

Sosio, R., Crosta, G. B. and Frattini, P.: Field observations, rheological testing and numerical modelling of a debris flow event, Earth Surf. Process. Landforms, 32, 290-306, 2007.

Sorooshain, S. and Gupta, V. K.: Automatic calibration of conceptual rainfall-runoff models: the question of parameter observability and uniqueness, Water Resour. Res., 19, 260-268, https://doi.org/10.1029/WR019i001p00260, 1983.

Stancanelli, L. M. and Foti, E.: A comparative assessment of two different debris flow propagation approaches – blind simulations on a real debris flow event, Nat. Hazards Earth Syst. Sci., 15, 735–746, https://doi.org/10.5194/nhess-15-735-2015, 2015.

Takahashi, T.: Debris flow IAHR Monographs, CRC Press, 1991.

Takahashi, T.: Mechanical characteristics of debris flow, J. Hydraul., 104, 8, https://doi.org/10.1061/JYCEAJ.0005046, 1978.

TELEMAC-2D User Manual, EDF-R&D, http://www.opentelemac.org, 2017.

Thielicke, W. and Sonntag, R.: Particle image velocimetry for Matlab: Accuracy and enhanced algorithms in PIVlab, J. Open Res. Softw., 9, 1, 12, https://doi.org/10.5334/jors.334, 2021.

US Army Corps of Engineers: HEC-RAS, River Analysis System, Hydrologic Engineering Center, Mud and Debris Flow, https://www.hec.usace.army.mil/confluence/rasdocs/rasmuddebris, 2023.

Voellmy, A.: Ueber die Zerstoerungskraft von Lawinen, Schweiz. Bauzeitung, 73, 159-162, 1955.

Wang, T., Yin, K., Li, Y., Xiao, C., Zhu, H. & Westen C. W.: Physical vulnerability curve construction and quantitative risk assessment of a typhoon-triggered debris flow via numerical simulation: A case study of Zhejiang Province, SE China, Landslides 21, 1333–1352, https://doi.org/10.1007/s10346-024-02218-8, 2024.

Wu, Y. H., Liu, K. F, Chen, Y. C.: Comparison between FLO-2D and Debris-2D on the application of assessment of granular debris flow hazards with case study. J. Mountain Res., 10, 293-304, https://doi.org/10.1007/s11629-013-2511-1, 2013.

Zegers, G., Mendoza, P. A., Garces, A., and Montserrat, S.: Sensitivity and identifiability of rheological parameters in debris flow modeling, Nat. Hazards Earth Syst. Sci., 20, 1919–1930, https://doi.org/10.5194/nhess-20-1919-2020, 2020.